Atmospheric Environment 98 (2014) 66–77

Contents lists available at ScienceDirect

Atmospheric Environment

journal homepage: www.elsevier.com/locate/atmosenv

Model evaluation of methods for estimating surface emissions and chemical lifetimes from satellite data

Benjamin de Foy [a, *], Joseph L. Wilkins [a], Zifeng Lu [b], David G. Streets [b], Bryan N. Duncan [c]

[a] Department of Earth and Atmospheric Sciences, Saint Louis University, St. Louis, MO, USA
[b] Decision and Information Sciences Division, Argonne National Laboratory, Argonne, IL, USA
[c] Atmospheric Chemistry and Dynamics Laboratory, NASA Goddard Space Flight Center, Greenbelt, MD, USA

HIGHLIGHTS

- Exponentially-Modified Gaussian fit yield accurate emissions by wind speed groups.
- EMG lifetime estimates need careful plume rotation and are biased low.
- 2D Gaussian fit can be sensitive to winds and domain choice.
- 2D Gaussian lifetime estimates are a measure of dispersion not chemistry.
- A new Inverse Radius fit yields improved results compared with the 2D Gaussian fit.

GRAPHICAL ABSTRACT

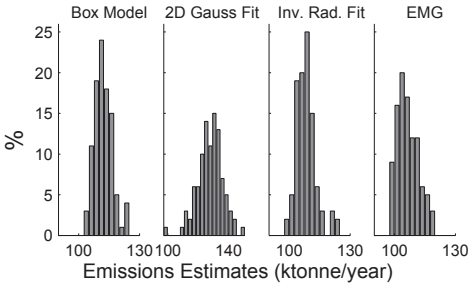

ARTICLE INFO

Article history:
Received 6 May 2014
Received in revised form
20 August 2014
Accepted 21 August 2014
Available online 23 August 2014

Keywords:
Emission inventory
Satellite retrieval
Chemical lifetime
Air quality model
Emissions estimation

ABSTRACT

Column densities from satellite retrievals can provide valuable information for estimating emissions and chemical lifetimes objectively across the globe. To better understand the uncertainties associated with these estimates, we test four methods using simulated column densities from a point source: a box model approach, a 2D Gaussian fit, an Inverse Radius fit and an Exponentially-Modified Gaussian fit. The model results were simulated using the WRF and CAMx models for the year 2005, for a single point source outside Atlanta in Georgia, USA with specified emissions and three chemical scenarios: no chemical reactions, 12 h chemical lifetime and 1 h chemical lifetime. No other sources were included in the simulations. We find that the box model provides reliable estimates irrespective of plume speed and plume direction, if the plume speed and the chemical lifetime are known accurately. The 2D Gaussian fit was found to be sensitive to plume speed and direction, and requires omnidirectional dispersion in order to have a decent fit. However, the 2D Gaussian fit is only an approximate fit to the data, and the discrepancies mean that the results are dependent on the geographical domain used for the optimization. An Inverse Radius fit is introduced to correct this issue, which is found to provide improved emissions and lifetime estimates. The Exponentially-Modified Gaussian fit also gave improved estimates. It is however dependent on accurate plume rotation such that reported chemical lifetimes with this method could be significantly underestimated.

1. Introduction

Extensive satellite remote sensing capabilities have led to a large increase in the understanding of global emissions and transport of air pollutants (Martin, 2008). These have been used in many

* Corresponding author.
E-mail address: bdefoy@slu.edu (B. de Foy).

http://dx.doi.org/10.1016/j.atmosenv.2014.08.051
1352-2310/

different settings where they can be viewed as part of a system that relies on the combination of remote sensing with ground-based measurements and numerical models in order to better understand atmospheric composition (Hoff and Christopher, 2009). As both satellite and modeling capabilities have improved, the ability to detect more local sources has greatly improved, to the point where the emissions of individual power plants can be routinely tracked from space (Streets et al., 2013, 2014). This capability will further increase with the future GEO-CAPE (Fishman et al., 2012) and TEMPO missions (Hilsenrath and Chance, 2013) which will be in geostationary orbit and provide expanded diurnal and spatial resolution.

Retrievals of NO_2 from the Global Ozone Monitoring Experiment (GOME) have been used to identify emissions from individual sources and cities using the standard swath mode (40 by 320 km^2) (Martin et al., 2003) and the narrow swath mode (40 by 80 km^2) (Beirle et al., 2004b). Data from the Ozone Monitoring Instrument (OMI) with a maximum resolution of 13 by 24 km^2 were used to create maps over the USA at 0.1° resolution that were used to compare NO_2 columns with measured surface concentrations (Lamsal et al., 2008). By oversampling the data from multiple swaths onto fine grids, de Foy et al. (2009) and Russell et al. (2010) obtained spatial maps with a resolution down to 3 km. This was used to identify the transport of SO_2 from a refinery and a volcano on either side of Mexico City (de Foy et al., 2009) and to identify the spatial extent of the weekday–weekend effect in four metropolitan regions in California (Russell et al., 2010). Valin et al. (2011) performed a simulation study to show that this kind of resolution is sufficient to determine NO_2 columns over point sources and to accurately model the NO_2 loss rate.

As described in the review articles cited above (Martin, 2008; Hoff and Christopher, 2009; Streets et al., 2013), many studies have used inverse models to estimate emissions on regional to global scales. An alternative approach has been to estimate emissions directly from the column densities using mass balance or curve fitting methods. This paper seeks to evaluate the potential of four of these methods to estimate emissions and chemical lifetimes of individual point sources. The four methods are: 1. a box model using simple mass balance, 2. a 2D Gaussian fit, 3. an Inverse Radius fit and 4. an Exponentially-Modified Gaussian fit.

The simplest method to use is a mass balance in a box containing the target source. This textbook method is described for example in chapter 3 of Jacob (1999). It was used to evaluate global NO_x emissions from GOME data by Leue et al. (2001) and Martin et al. (2003). The method relies on a critical parameter α, which relates column densities to emission rates and consists of a scaling factor divided by the residence time of the pollutant in the box. In Martin et al. (2003) it was obtained empirically from model simulations. This method has been widely used, for example for estimating sources of NO_x over India (Lu and Streets, 2012; Ghude et al., 2013). Carn et al. (2007) followed this approach to determine emissions of SO_2 from copper smelters in Peru using data from the Ozone Monitoring Instrument (OMI), and Lee et al. (2011) evaluated global SO_2 emissions with it.

Duncan et al. (2013) make use of the fact that NO_x emissions from US power plants are known from in-stack Continuous Emission Monitoring Systems (CEMS) to estimate the value of the parameter relating the emissions to the OMI column densities. This is the equivalent of using the mass balance in Martin et al. (2003) to identify the parameter α from known emissions, rather than determining the emissions from a model-specified value of α. In the supplementary material, they show that the lifetime is a combination of the dispersion lifetime and the chemical lifetime, with the dispersion term being the dominant one for the 0.3 by 0.3° domains used in the analysis. In this study we use the wind speed to estimate the dispersion time, and the a priori chemical lifetime specified in the inputs.

In related work, Lamsal et al. (2011) use a non-dimensional parameter β to relate the normalized change in column densities to the normalized change in emissions, and hence to study changes in emissions over time. In this case, β is required to account for changes in chemical lifetimes as a function of changing chemical burdens in the atmosphere. As an example, β was used to obtain estimates of emissions in European shipping routes (Vinken et al., 2014). In our work we are dealing with constant chemical lifetimes and hence a β of one.

The 2D Gaussian fit was introduced by Fioletov et al. (2011) to estimate the change in emissions of large SO_2 point sources along the Ohio River Valley. The constant of proportionality between the fit parameters and the actual emissions was determined empirically from the known emissions of the sources. Fioletov et al. (2013) extended the work to compare results of the method for different satellite instruments, and concluded that the improved resolution of OMI led to better emissions estimates than the other sensors. Lu et al. (2013) found an excellent match between the 2D Gaussian fit and emissions inventories for large SO_2 sources in India. The analysis was used to show the increase in emissions from 2005 to 2012 resulting from the increased column densities in OMI.

Leue et al. (2001) used GOME data to estimate the emissions and lifetime of NO_x from the East Coast of the USA by assuming linear transport with an exponential decrease of column densities with distance from the coast. Following Leue et al. (2001), Beirle et al. (2004a) used an Exponentially-Modified Gaussian fit to estimate the emissions and lifetimes of NO_2 from the shipping lane between Sri Lanka and Indonesia, and Beirle et al. (2011) used it to estimate the emissions and lifetimes of NO_2 from Riyadh, Saudi Arabia and other cities around the world. Maps of NO_2 column densities from OMI were grouped by wind direction, and line densities were obtained by summing the columns in the direction perpendicular to the winds. From the fit, the emissions and the lifetime were obtained. In particular, the lifetimes were found to be around 4 h for most locations in the low and mid-latitudes. Valin et al. (2013) adopted the same approach but introduce plume rotation in order to be able to classify the column density maps by wind speed and preserve a representative sample size. The results suggest that the chemical lifetime is a function of wind speed, with longer lifetimes of 7–8 h at weak wind conditions, down to 5.5 h for faster winds. Overall, Valin et al. (2013) show the importance of distinguishing the meteorological variability from the chemical variability in order to improve estimates of plume chemistry, and more specifically of OH concentrations in the plume.

In this paper we evaluate different methods for estimating the emissions and chemical lifetimes from column densities by using exclusively numerical simulations with pre-determined emission rates and chemical lifetimes. Section 2.1 describes the simulations and Sections 2.2–2.5 present the estimation methods. In Section 3.1, we present the meteorological simulations and compare them with observations in order to establish their statistical adequacy for representing actual wind transport conditions. Section 3.2 presents the results of the estimation methods using synthetic winds which provide a simplified case, and Section 3.3 shows the results from the year-long WRF simulations for 2005 which provide a more realistic approximation of atmospheric dispersion.

2. Methods

2.1. Numerical simulations

The meteorological simulations were performed with the Weather Research and Forecasting (WRF) model (Skamarock et al.,

2005), and use the North American Regional Reanalysis (Mesinger et al., 2006) for the initial and boundary conditions. WRF version 3.4 was run on 2 domains with 27 and 9 km horizontal resolution and 40 vertical levels. Fig. 1 shows a map of the 2 domains.

The model was run with two-way nesting, with the Yonsei University (YSU) boundary layer scheme, the Kain–Fritsch convective parameterization, the NOAH land surface scheme, the WSM 3-class simple ice microphysics scheme, the Goddard shortwave scheme and the Rapid Radiation Transfer Model longwave scheme. 74 individual simulations were performed to cover the entire year of 2005. Each simulation lasted 162 h, of which the first 42 h were considered spin-up time and the remaining 5 days were used for analysis. The simulation set-up is similar to the one used for inverse modeling in de Foy et al. (2014b) and de Foy et al. (2014a), where it was shown to be able to identify emissions inventory information.

The Comprehensive Air-quality Model with eXtensions (CAMx v5.40, ENVIRON (2011)), an Eulerian 3D grid model, was used to obtain hourly concentrations from a location representative of a large power plant to the northwest of Atlanta, see Fig. 1. The simulated stack was 305 m tall, 7.6 m in diameter, and had an exit velocity of 21 m/s and exit temperature of 130 °C. The simulated emissions were 100 ktonne/yr.

Simulations were made using the same two nested domains as the WRF model, and with zero background concentrations. The base case simulation was made for a passive tracer with no-chemistry scheme. Two further simulations were made using exponential decay (mechanism 10 in CAMx): one with a chemical lifetime of 12 h and the other with a chemical lifetime of 1 h. In this way, we could test the accuracy of the lifetime estimates from the different estimation methods. We selected 1 and 12 h to bracket different actual lifetimes encountered in the atmosphere. Tests were also performed with a 6 h lifetime, but as these do not change the conclusions they are not presented here. For a median wind speed of 5 m/s, a non-reacting plume would take approximately 15 h to leave the fine domain, and 3 h to travel from the center to the edge of the 100 km domain used by the methods below.

In addition to simulations representing the meteorology of 2005, we performed CAMx simulations for one month with synthetic westerly winds of 5 m/s. This serves to test the methods while removing all uncertainty due to transport.

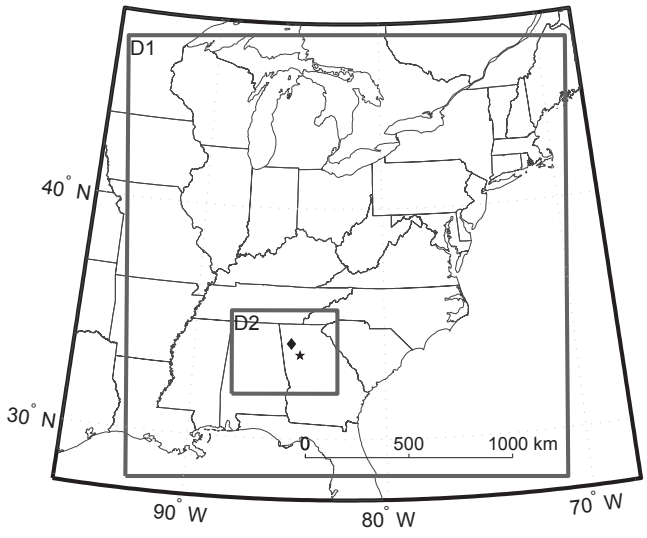

Fig. 1. WRF Domains 1 and 2 used for the simulations. Black diamond shows the source site, black star shows the location of the meteorological site (KATL).

Gridded column data were calculated for 2 pm Eastern Standard Time everyday to be used as input to the emissions estimation methods. This time was chosen as it coincides approximately with the overpass of the OMI instrument on-board the Aura satellite.

Column density data on the 9 km CAMx grids were oversampled to 2 km grids centered on the source point as described in de Foy et al. (2009). This was done so that the results using model data would be comparable to testing the methods on oversampled satellite data.

Some of the methods assume a single plume direction while others work better with plume dispersion in all directions. The synthetic winds have a single wind direction, and it is straightforward to create an omnidirectional dispersion case by rotating each day by a different increment. The WRF simulations disperse in all directions, and we need to identify the plume direction in order to create cases with uniform eastward dispersion. This was done by calculating the moments of inertia of the plume vertical column densities and hence determining the principal axes of rotation. The CAMx grids were then rotated using the angle of the principal axis before oversampling to the finer 2 km grid. Separate tests were performed by rotating the column densities using the WRF wind direction at the source, but this was not found to be as effective as using the plume principal axis.

As we will see in the following sections, all the methods require an estimate of the plume dispersion speed. The emissions estimate is a linear function of this speed, and so any errors in the speed will directly translate into errors in the emissions estimate. For this work, we use the average wind speed in the bottom four layers of the WRF model, which corresponds to approximately the first 360 m above ground level.

2.2. Box model

The simplest method for evaluating emissions from column densities is to use a box model that includes the source of interest, as described for example in chapter 3 and problem 3.6 of Jacob (1999). For this method, we are using a single value of average column density, and therefore we can derive a single parameter of emissions strength. The chemical lifetime needs to be included as an input into the model. If we assume a box is in steady-state, the emissions rate (E) of a substance into that box is equal to the mass of substance (M) in the box divided by the residence time (τ) of the substance in the box (see supplementary material in Duncan et al. (2013) for more details):

$$E = \frac{M}{\tau} \tag{1}$$

The mass of substance in the box is obtained from the average column density $\mathrm{Col}_{\mathrm{av}}$ in the box as: $M = f\Delta x\,\Delta y\,\mathrm{Col}_{\mathrm{av}}$, where f is a scaling factor to keep the units consistent. Because of the way we calculate the dispersion lifetime below, the source must be located in the middle of the box.

The residence time is given by the combination of the dispersion time τ_{d} and the chemical reaction time τ_{c}:

$$\frac{1}{\tau} = \frac{1}{\tau_{\mathrm{d}}} + \frac{1}{\tau_{\mathrm{c}}} \tag{2}$$

With this method, we cannot determine the chemical reaction time from the model. Instead, it needs to be estimated a priori, and included into Eq. (2) in order to obtain the emissions. As a consequence, any uncertainty in the chemical lifetime will add to the uncertainties in the emissions estimates. The dispersion lifetime can be estimated by considering a source that is in the middle of a box of dimensions Δx by Δy:

$$\tau_d = \frac{\Delta x}{2U} \tag{3}$$

where U is the speed of the plume in the box. In this way, we obtain the equivalent of α in Eq. (3) of Martin et al. (2003).

As noted above, Lamsal et al. (2011) related normalized differences in emissions to normalized differences in column densities using a non-dimensional parameter β, which can be expressed as follows:

$$\frac{\Delta E}{E} = \beta \frac{\Delta \Omega}{\Omega} = \beta(r-1) \tag{4}$$

where E represent the emissions and Ω the column densities. ΔE represents the change from time 1 to time 2 and the ratio of the column densities is given by: $r = \Omega_2/\Omega_1$.

Using the box model above, we can develop a separate expression for the normalized difference in emissions as follows:

$$\frac{\Delta E}{E} = \frac{\tau_1}{\tau_2}\left(r - \frac{\tau_2}{\tau_1}\right) \tag{5}$$

Although there is not a direct match between Eqs. (4) and (5), we can see how for small changes in τ, β will be inversely proportional to the change in the lifetime parameter τ_2/τ_1, which is to say that a value of β greater than one corresponds to decreasing chemical lifetimes in the atmosphere. In this study we use constant chemical lifetimes, which is the equivalent of using $\beta = 1$, and focus on Eqs. (1) and (2) to obtain emissions estimates.

2.3. 2D Gaussian fit

An alternative method to the box model is to assume that the column density surrounding an isolated source will have a two dimensional Gaussian shape when averaged over a sufficiently long time period. This was suggested for large point sources of sulfur dioxide by Fioletov et al. (2011), with the following equation:

$$\mathrm{Col}_{\mathrm{fit}}(x,y) = \frac{a}{2\pi\sigma_x\sigma_y\sqrt{1-\rho^2}} \exp\left(-\frac{1}{2(1-\rho^2)} \left[\frac{(x-\mu_x)^2}{\sigma_x^2} + \frac{(y-\mu_y)^2}{\sigma_y^2} - \frac{2\rho(x-\mu_x)(y-\mu_y)}{\sigma_x\sigma_y} \right] \right) \tag{6}$$

In this equation, μ_x and μ_y are included to determine the center of the 2D Gaussian fit. σ_x, σ_y determine the length scale of the Gaussian curve in the x and y directions, and ρ is a rotation parameter for the ellipse defined by σ_x, σ_y. The integral of $\mathrm{Col}_{\mathrm{fit}}$ over x and y is equal to a which represents the mass of substance near the source.

Using a single value for the dispersion length scale, $\sigma = \sqrt{\sigma_x^2 + \sigma_y^2}$, and a representative wind speed, U, it is possible to convert the length scale obtained from the 2D Gaussian fit into a time scale:

$$\tau = \frac{\sigma}{U} \tag{7}$$

We can now convert a to a mass amount M and use Eq. (1) to obtain an estimate of the emissions from the source. With this method, we do not need to specify the time scale and we can make use of as much spatial data as we have to obtain the 2D Gaussian fit. Nevertheless, the estimate is not based on a physical description of the processes transporting the plume. In particular there is no way to differentiate between the impact of dispersion and the impact of chemical reactions.

2.4. Inverse Radius fit

We now develop an alternative to the 2D Gaussian fit for the purposes of comparing that fit with an idealized solution to the dispersion equations. If we use a physical approach and assume omnidirectional dispersion from a point source, then we expect the column densities to follow an Inverse Radius relationship: in the absence of chemical reactions, as a substance spreads from the source, the circumferential integral remains constant and is proportional to the strength of the source. An exponential term can be included to account for chemical reactions, leading to the following equation:

$$\mathrm{Col}_{\mathrm{fit}}(x,y) = a \frac{r_{\min}}{\max(r, r_{\min})} \exp\left(-\frac{r}{U\tau_c}\right) \tag{8}$$

where r is the distance from the center of the fit (given by μ_x and μ_y as for the 2D Gaussian fit). $r_{\min}$ is a free parameter to prevent the fit from breaking down close to the source. It is determined by the optimization routine and is usually between 1 and 5 km.

To account for spatial smoothing, we apply Gaussian smoothing in the x and y directions separately. The smoothing parameters are free parameters in the optimization routine, and were usually around 5 km for the 2 km grid cells used in this study. The Inverse Radius fit can be used as an alternative to the 2D Gaussian fit on a spatial map of column densities around a source.

2.5. Exponentially-Modified Gaussian fit

An alternative physical approach to the Inverse Radius fit can be obtained by considering line densities in one dimension. We start with a standard Gaussian plume moving from west to east along the x-axis (Sutton, 1932). We integrate in the vertical to obtain column densities, and then we integrate these column densities along the y-axis to obtain line densities as a function of x:

$$L(x) = \sum_{-y_l}^{y_l} \mathrm{Col}(x,y)\Delta y \tag{9}$$

where y_l determines the distance over which to sum the column densities and is chosen to include most of the mass of the plume.

In the absence of deposition and chemical reactions, and with no smoothing in the x direction, this yields a step function, with the step taking place at the point of emission, and the height of the step being proportional to the mass of substance in the plume. Given these assumptions, integrating column densities from satellite data perpendicular to the wind direction should yield this same step function.

In practice, there is smoothing in the wind direction because the point source is not a perfect point and because there is mixing in the x direction as much as in the y direction. This smoothing can be represented by a Gaussian function (g) in the x direction with the smoothing length scale given by σ_x.

We also wish to include chemical decay in the model, and so we use an exponential decay function (e) in x to simulate this using a length scale for chemical decay x_o. μ_x is included to determine the location of the plume, as was done for the 2D Gaussian fit above. The theoretical profile is obtained by the convolution of the exponential function and the Gaussian function, as described in Beirle et al. (2011):

$$e(x) = \exp\left(-\frac{x-\mu_x}{x_o}\right) \quad \text{for } x \geq \mu_x, 0 \text{ otherwise} \tag{10}$$

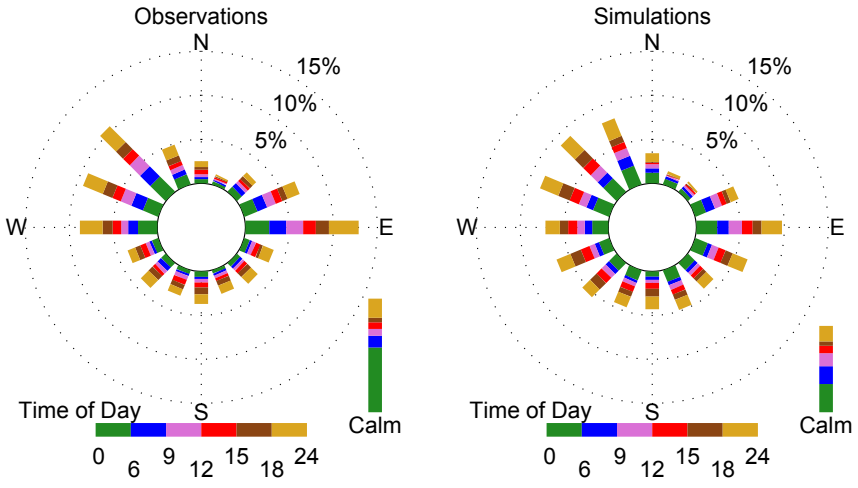

Fig. 2. Wind roses by time of day for Atlanta Hartsfield International Airport (KATL) using 2005 hourly data: observations (left) and WRF simulations (right).

$$g(x) = \frac{1}{\sqrt{2\pi}\sigma_x}\exp\left(-\frac{x^2}{2\sigma_x^2}\right) \tag{11}$$

$$L_{\text{fit}}(x) = a \cdot (e \otimes g)(x) \tag{12}$$

where a is the amount of mass M in the plume over the interval x_o.

This gives the following equation for the line density:

$$L_{\text{fit}}(x) = \frac{a}{2}\exp\left(\frac{\sigma_x^2}{2x_o^2} - \frac{x-\mu_x}{x_o}\right)\left(1 - \text{erf}\left(\frac{\sigma_x^2 - x_o(x-\mu_x)}{\sqrt{2}\sigma_x x_o}\right)\right) \tag{13}$$

In this equation, we can use a representative plume transport speed U to convert length scales to time scales, and hence we can obtain the emission rate and the lifetime as follows:

$$E = Ua \tag{14}$$

$$\tau = \frac{x_o}{U} \tag{15}$$

If the transport speed is uniform, the direction is constant, and in the absence of deposition, this should give us an accurate estimate of the emissions and of the chemical lifetime based on line densities along the transport direction. In order to satisfy the directional requirement, we rotate all the plumes to have maximum column densities in the same direction, as recommended by Valin et al. (2013).

In practice, we use the optimization routine "fmincon" in MATLAB to determine an optimal set of parameters based on the line densities from the plume simulations described in Sec. 2.1. Constraints in the routine are used to prevent unphysical negative values for a, x_o and σ_x.

3. Results & discussion

3.1. WRF and CAMx simulations

In order to evaluate the meteorological conditions and the representativeness of the WRF simulations, we present a comparison of wind speed and direction, temperature and humidity from the model results with observations from Atlanta Hartsfield

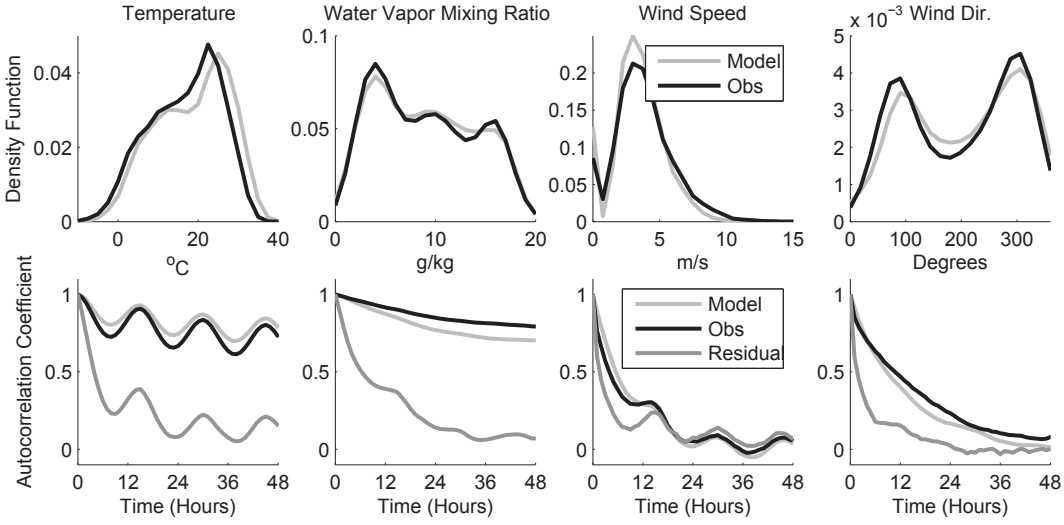

Fig. 3. Probability density function of observed and simulated temperature, water vapor, wind speed and wind direction at KATL (top) along with autocorrelation coefficients of observations and simulations as well as of the residual between the two (bottom).

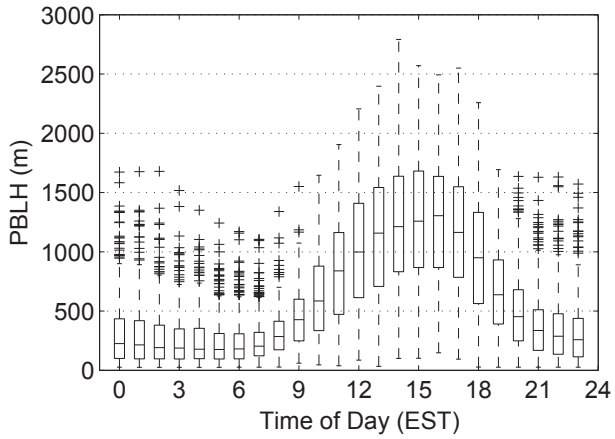

Fig. 4. Diurnal profile of the Planetary Boundary Layer Height (PBLH) simulated by WRF at KATL for 2005.

International Airport (KATL). The data were obtained from the Integrated Surface Hourly Database from the National Climatic Data Center. In order to make direct comparisons, we classify all WRF winds with speeds below 1.5 m/s as calms.

Fig. 2 shows surface wind roses by time of day at KATL from the measurements and from WRF. This shows that the model correctly captures the main features of the flow, with dominant wind directions from the northwest and from the east, and with approximately 10% of hours experiencing calm winds.

Fig. 3 shows the probability density function for the observations and the simulations. The distributions passed the Kolmogorov–Smirnov test to lower than the 1% significance level for temperature, wind speed and direction, and to lower than the 5% level for specific humidity. Pearson's correlation coefficient was 0.97 for temperature, 0.94 for specific humidity, 0.61 for wind speed and 0.86 for wind direction. The most significant model bias is for temperature with a warm bias of 1.9 °C in the model. The autocorrelation plots show similar behavior in the model and in the observations, and show that the autocorrelation time of the model residual is much lower than 24 h. This shows that the simulations are statistically representative of the local surface conditions, as was shown for Milwaukee in de Foy et al. (2014b).

Finally we show the diurnal profile of the boundary layer height at KATL in Fig. 4. This shows that stable conditions prevail at night with median heights around 200 m, followed by median mixing heights of 1250 m in the afternoon and maximum heights on some days above 2500 m.

Overall, we see that the conditions at KATL are representative of mid-latitude cities. The plume dispersion patterns under these conditions will be in all directions with predominant flow to the southeast and to the west. Furthermore, we see that the simulations from the WRF model correctly represent the local meteorology and can therefore be used to generate representative fields of plume dispersion.

Fig. 5 shows the average column densities for the three different chemical scenarios for both the un-rotated (original) plumes and the rotated plumes. This confirms that despite the predominant wind directions there is enough wind variation to have dispersion in all directions over the course of the year-long simulation. Rotation by plume direction yielded an average eastward plume with only minor spreading in the north–south direction. As expected, the horizontal extent of the plume is determined by the chemical lifetime of the plume: without reactions, the plume is still clearly visible 100 km from the source, with 1-h chemistry it lasts less than 50 km.

3.2. Estimates with synthetic meteorology

Table 1 shows the estimated emissions and chemical lifetimes for the case with the steady 5 m/s eastward winds for all four methods. The box model was found to be relatively insensitive to the size of the domain, and was applied to a square domain that was 100 km wide. This yielded estimates within 10% of the model-specified value for the case with no chemical reactions, and overestimated by nearly 20% in the case with 1-h chemistry. The method does not depend on the rotation of the plume, although for these particular cases, using omnidirectional dispersion gave larger estimates than using eastward plumes.

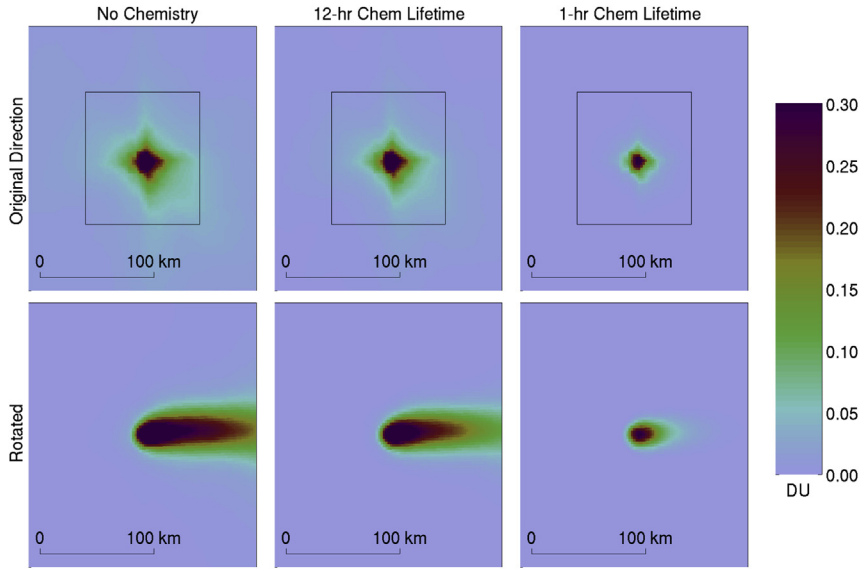

Fig. 5. Annual average columns for 2005 with no-chemistry (left), 12-h (middle) and 1-h (right) chemical lifetimes. The 9 km model output was resampled to 2 km grids for parameter estimation. The top row shows averages of the plumes in the original directions. The bottom row shows the average of the plumes rotated to have maximum column densities towards the east.

Table 1
Emissions and chemical lifetime estimates from the synthetic winds case using the box model, the 2D Gaussian fit, the Inverse Radius fit, and the Exponentially-Modified Gaussian fit (EMG). "Eastward Plumes" have steady 5 m/s winds towards the east. Omnidirectional dispersion cases were obtained by rotating the eastward plumes in all directions. Boldface shows the best estimates, model-specified emissions were 100 ktonne/yr.

Plume Direction	Chemical	Box model	2D Gaussian fit		Inv. Radius fit		EMG fit	
	Lifetime hours	Emissions ktonne/yr	Emissions ktonne/yr	Lifetime hours	Emissions ktonne/yr	Lifetime hours	Emissions ktonne/yr	Lifetime hours
Eastward	∞	93.7	171.5	3.4	587.4	0.4	**99.0**	**424.7**
Omnidirectional	∞	105.0	**120.0**	1.2	**95.6**	**2122.4**	305.3	0.7
Eastward	12	102.7	155.8	2.8	711.4	0.3	**99.2**	**11.4**
Omnidirectional	12	113.6	**119.2**	1.2	**111.7**	**12.0**	299.8	0.7
Eastward	1	116.4	124.3	0.7	652.7	0.1	**97.8**	**1.0**
Omnidirectional	1	118.4	**80.0**	0.8	**102.8**	**1.1**	195.1	0.4

The 2D Gaussian fit assumes that the plume is dispersing in all directions. Consequently, it did not fit the eastward plume cases properly and overestimated the emissions by nearly a factor of 2 (see Table 1). This method must therefore be applied to plumes with dispersion in all directions. Fig. 6 shows cross-sectional sums of the data and the fit for a domain that is 100 km wide. Although the 2D Gaussian fit approximates the data, it does not match it perfectly. This leads to a domain dependence of the results. With the 100 km domain the emissions were overestimated by 20% for the slow chemistry cases, and underestimated by 20% for the fast chemistry case. The lifetimes estimated by this method were 1.2 h for the slow chemistry cases and 0.8 h for the fast case. This shows that the method basically estimates a dispersion lifetime within the fit domain and is only weakly sensitive to chemical reaction times.

The bottom row of Fig. 6 contains the results of the Inverse Radius fit showing that there is nearly a perfect fit of the data to the analytical model for the cases with omnidirectional dispersion. The results of the method are therefore less sensitive to domain choice, and are more accurate: emissions were within around 10% of the model-specified value, as shown in Table 1. The lifetimes were also much more accurate and representative of the chemical lifetimes: 2122 h is effectively the same as infinity for the case with no-chemistry, 12.0 h for the 12-h chemistry case, and 1.1 h for the 1-h chemistry case. As with the 2D Gaussian fit however, the Inverse Radius fit assumes omnidirectional dispersion and fails for the eastward plume cases.

The emissions estimate from the Exponentially-Modified Gaussian (EMG) fit were excellent using the eastward plumes, with less than 3% errors for all three chemistry cases (see Table 1). Likewise, the lifetime estimates were also very close to the model-specified value. A chemical lifetime of 570 h for the case without chemistry is effectively infinite for the local scale considered here. The lifetime estimate was 11.4 h for the 12-h case, and 1.0 h for the 1-h case.

Fig. 7 shows the line density of the input data and of the fit. Thanks to the quality of the fit, this method is much less sensitive to the domain chosen than the 2D Gaussian fit. The excellent match between the two curves shows that the EMG fit is an accurate analytical model for plume dispersion so long as the plume is rotated accurately. The method fails totally in the omnidirectional dispersion case, as can be seen in Table 1. In fact, it was found to be sensitive to the quality of the plume rotation. In particular, small discrepancies in rotational direction had large impacts on the lifetime estimates making them much shorter than they should be.

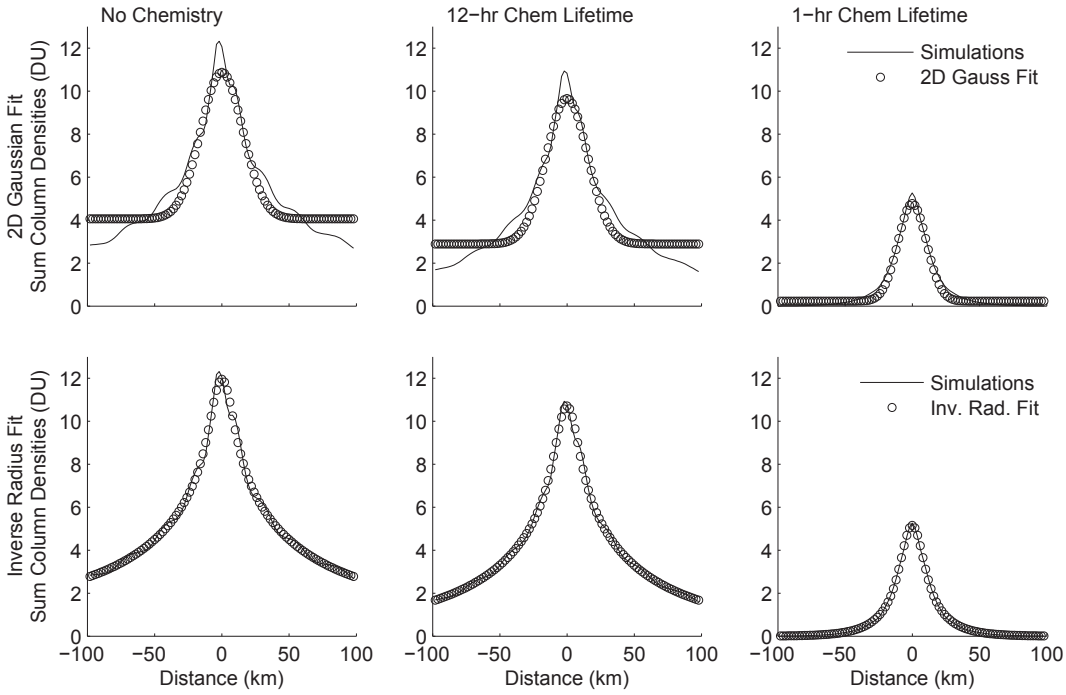

Fig. 6. Sum of the cross-sections along the *y*-axis for the synthetic case with omnidirectional plume rotation for the no-chemistry case (left), 12-h chemistry (middle) and 1-h chemistry (right). Top row shows the 2D Gaussian fit overlayed on the model data, bottom row shows the Inverse Radius fit overlayed on the model data.

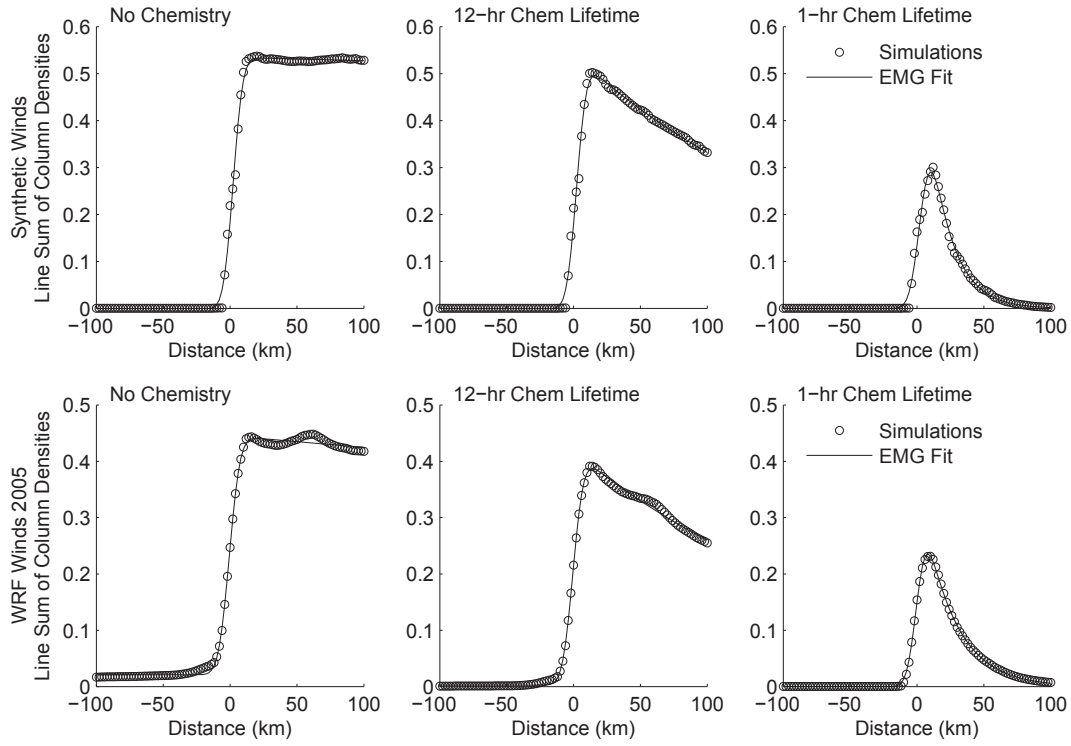

Fig. 7. Line densities (sum of DU along the *y*-axis) with eastward transport for the no-chemistry case (left), 12-h chemistry (middle) and 1-h chemistry (right). The Exponentially-Modified Gaussian fit is overlayed on the data from the synthetic case (top row) and from the WRF simulations for 2005 (bottom row).

In summary, the synthetic tests show that the box model gave decent estimates of the emissions if the correct chemical lifetime was used in the model, and this irrespective of the plume direction. The 2D Gaussian fit requires omnidirectional plume dispersion. The lifetimes however were very short, and represented the dispersion lifetime rather than the chemical lifetime. The method was also sensitive to domain choice. These problems were fixed using the Inverse Radius method which gave more accurate and robust estimates of the emissions as well as accurate estimates of the chemical lifetime. Finally, the EMG fit gave excellent emissions and lifetime estimates if the plume was accurately rotated to be always eastward. Furthermore, the method was robust across the three chemical lifetime cases.

3.3. Estimates with 2005 WRF meteorology

Table 2 shows the estimated emissions and chemical lifetimes using the meteorological fields simulated by WRF for 2005. Based on the tests with the synthetic meteorology, we present the results for the omnidirectional dispersion cases for the box model, the 2D Gaussian fit, and the Inverse Radius fit, and for eastward plumes for the EMG fit. In addition to presenting the results for the average of all 365 days in the year, we present results by quartiles according to wind speed category for Calm (0–25%), Weak (25–50%), Medium (50–75%) and Strong (75–100%) winds. Each category has either 91 or 92 members. The "All" wind group has the largest range of wind speeds, and therefore the averages are the result of combining

Table 2
Emissions and chemical lifetime estimates from the WRF winds for 2005 using the box model, the 2D Gaussian fit, the Inverse Radius fit, and the Exponentially-Modified Gaussian fit (EMG). The box model, 2D Gaussian fit and Inverse Radius fit are applied to the annual average of the columns, the EMG fit uses the average of plumes rotated to all be eastward. Boldface shows the best estimates, model-specified emissions were 100 ktonne/yr.

Chemical Lifetime hours	Winds	Wind speed		Box model	2D Gaussian fit		Inv. Radius fit		EMG fit	
		Min m/s	Max m/s	Emissions ktonne/yr	Emissions ktonne/yr	Lifetime hours	Emissions ktonne/yr	Lifetime hours	Emissions ktonne/yr	Lifetime hours
∞	All	0	15.4	130.2	184.2	0.8	143.9	18.9	116.9	17.3
∞	Calm	0	3.0	78.1	**130.1**	1.8	110.5	19.2	73.9	21.9
∞	Weak	3.0	5.0	**106.2**	137.9	1.2	109.7	37.4	**102.2**	17.4
∞	Medium	5.0	7.3	**105.8**	139.2	0.8	109.1	36.6	95.4	91.5
∞	Strong	7.3	15.4	112.6	**131.3**	0.5	**107.0**	**7952**	106.7	**2782**
12	All	0	15.4	122.6	171.1	0.7	155.6	5.0	109.4	6.2
12	Calm	0	3.0	88.3	**115.9**	1.6	**111.4**	7.2	69.1	9.6
12	Weak	3.0	5.0	**107.1**	131.6	1.1	126.0	6.9	**96.8**	7.2
12	Medium	5.0	7.3	**106.8**	135.2	0.8	121.6	7.0	93.6	**9.5**
12	Strong	7.3	15.4	**110.0**	131.3	0.5	**116.9**	**7.8**	**97.0**	15.2
1	All	0	15.4	112.0	99.3	0.5	107.8	0.9	80.3	1.1
1	Calm	0	3.0	**99.4**	54.6	1.1	67.7	1.4	52.4	1.7
1	Weak	3.0	5.0	109.2	78.5	0.7	92.6	1.1	72.8	1.2
1	Medium	5.0	7.3	114.4	**94.1**	0.5	**104.9**	**1.0**	82.3	1.1
1	Strong	7.3	15.4	118.9	129.3	0.7	123.9	0.9	**88.0**	**1.0**

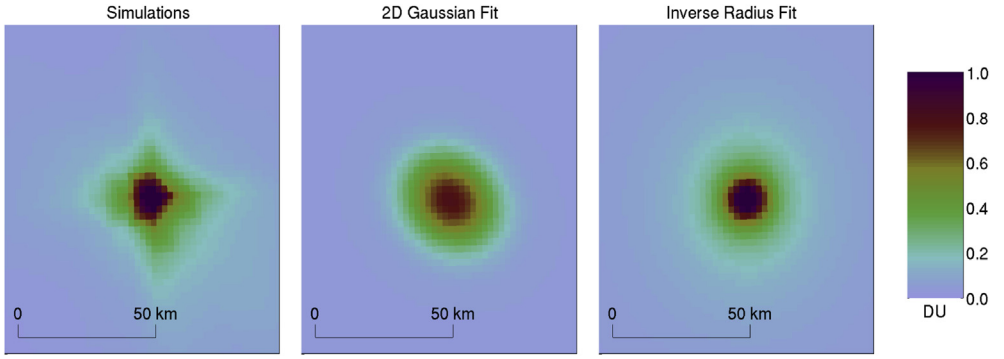

Fig. 8. 2D map of the plume dispersion for the no-chemistry case using the 2005 WRF winds. Left: Simulations, Middle: 2D Gaussian fit, Right: Inverse Radius fit.

members that are more dissimilar to each other than those in the four quartile groups. This results in larger estimation errors for this group, and so these will be excluded from the discussion below.

Depending on the wind speed category, the box model gave estimates that ranged from 78.1 to 118.9 ktonne/yr and were mostly within 10–20% of the model-specified value. The estimates are usually biased low for the Calm winds and biased high for the Strong winds with the Weak and Medium wind cases yielding the more reliable estimates.

Fig. 8 shows the 2D Gaussian fit next to the model data for the entire year with no-chemistry. The method yielded estimates that ranged from 55 to 140 ktonne/yr (see Table 2). Most of the estimates were biased high, except for the Calm and Weak winds with 1-h chemistry which were significantly underestimated. In terms of lifetime, the behavior of the estimate was the same as for the synthetic case, with lifetimes below 2 h representing the rapid dispersion from the source rather than the chemical reaction in the plumes. Sums of the cross-sections of the fit are shown in Fig. 9. While there is a good fit between the data and the emissions model, the figure shows that the 2D Gaussian fit is not a perfect match for the data as was discussed for the synthetic case above. This leads to discrepancies in the estimates and to dependencies on the size of the model domain chosen for the fit.

The map of the Inverse Radius fit is shown for the no-chemistry case in Fig. 8, and the cross-sectional sums are shown in the bottom row of Fig. 9 for the three chemistry cases. This shows clearly the improved match of the Inverse Radius fit with the data. The method led to emissions estimates ranging from 68 to 126 ktonne/yr and to lower errors than the 2D Gaussian fit. The lifetime estimates were much improved over the 2D Gaussian fit with values for the no-chemistry case of 8000 h for the Strong wind group and 37 h for the Weak and Medium wind groups. Bearing in mind that the reaction constant is the inverse of the lifetime suggests that these values are an accurate representation of the model-determined values. For the 12-h chemistry simulations, the lifetime estimates were between 7 and 8 h, and for the 1-h chemistry simulations they were between 0.9 and 1.4 h. Whereas the synthetic cases had nearly exact chemical lifetime estimates, this shows that in real cases the estimated chemical lifetime can be significantly shorter than the model-specified value.

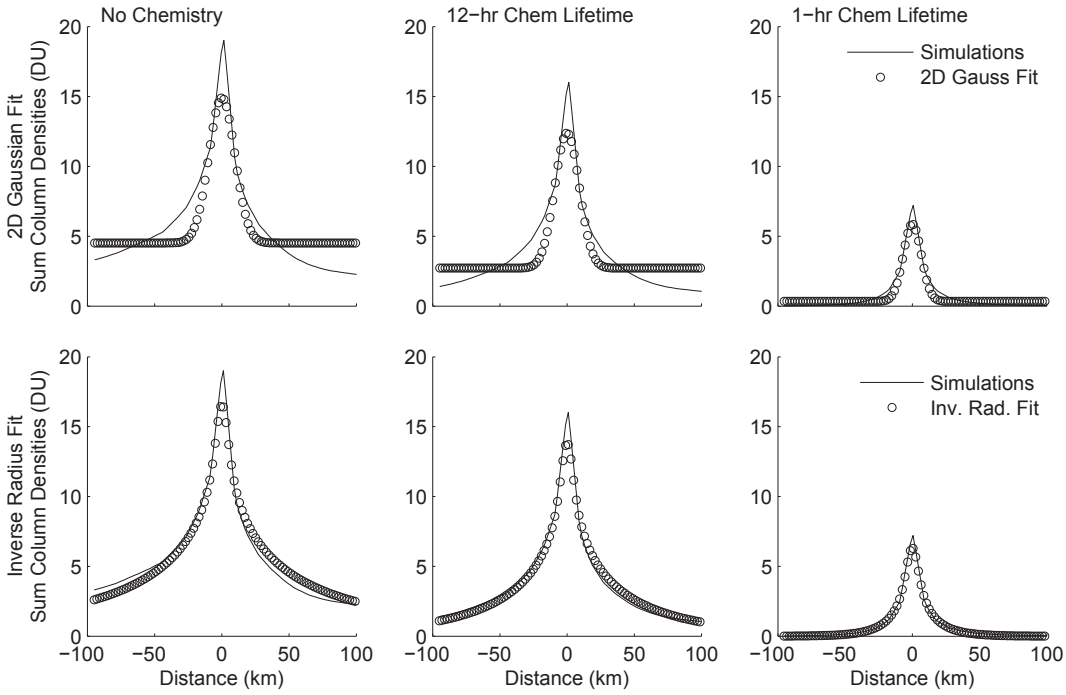

Fig. 9. Sum of the cross-sections along the *y*-axis using the 2005 WRF winds with omnidirectional plume rotation for the no-chemistry case (left), 12-h chemistry (middle) and 1-h chemistry (right). Top row shows the 2D Gaussian fit overlayed on the model data, bottom row shows the Inverse Radius fit.

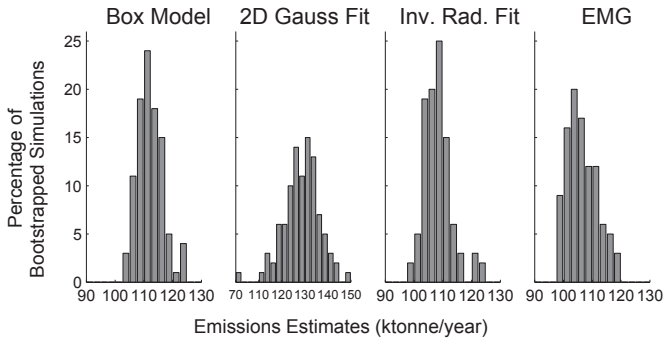

Fig. 10. Histogram of bootstrapped emissions estimates from the box model, the 2D Gaussian fit, the Inverse Radius fit, and the Exponentially-Modified Gaussian fit using the Strong winds quartile (7.3–15.4 m/s) from the 2005 WRF winds.

The EMG fit yielded the best emissions estimates of the four methods with a range of 73–107 ktonne/yr for the Weak, Medium and Strong wind groups, as shown in Table 2. Fig. 7 shows the data and the fit for the Medium wind speed cases. As in the synthetic case, the EMG model provides an excellent fit with the data which explains why this model gave the best results.

For the no-chemistry and 12-h chemistry cases, the emissions estimates were mostly within 5–10% of the model-specified values, whereas for the 1-h chemistry case the emissions were underestimated by 15% or more. The Calm wind group gave very low emissions estimates which suggest that this method should not be used with low wind speeds. In terms of lifetimes, the EMG estimates ranged from 17.4 to 2800 h for the no-chemistry case, 7.2 to 15.2 h for the 12-h case and 1.0 to 1.7 h for the 1-h case. The best estimates were from the Medium and Strong wind groups.

To test for the sensitivity of the EMG estimates to the accuracy of the plume rotation, we performed additional estimates using the WRF wind direction at the source to rotate the plume instead of rotating the plume in the direction of largest column densities. This did not degrade the emissions estimate substantially, but led to much shorter lifetimes: down to 6 h for the no-chemistry case and down to 4 h for the 12-h chemistry case. This suggests that the lifetime estimate includes a component from wind dispersion that can easily dominate the chemical lifetime estimate.

As a further test of uncertainty, we use bootstrapping to evaluate the sensitivity of the estimates to the selection of days in the wind speed groups. Within each wind speed group, individual maps of column densities were chosen at random with replacement in order to obtain bootstrapped average column densities. This procedure was repeated 100 times in order to characterize the uncertainty in the estimates.

Fig. 10 shows the histogram of the emission estimates for the no-chemistry case for all four methods with the Strong wind group. This shows that there is a standard deviation of around 5% of the mean estimate for the box model, the Inverse Radius fit and the EMG fit, and of around 10% for the 2D Gaussian fit.

In summary, the uncertainty in emissions due to using different wind speed groups is 20% or more of the model-specified input, and the uncertainty due to selection of individual days is approximately 10% for the 2D Gaussian fit and around 5% for the other three methods. Table 3 summarizes the strengths and weaknesses of the methods evaluated in this paper. The box model was found to be relatively robust so long as the chemical lifetime is known. The 2D Gaussian fit was found to be biased high for the case with no chemistry. The estimates are sensitive to the chemical lifetime however, with significant low biases for the 1-h chemistry case. The lifetimes estimated by the 2D Gaussian fit are dominated by the short plume dispersion lifetimes, such that the results are not indicative of plume chemistry. The agreement between the 2D Gaussian fit and the data has significant discrepancies which suggests that there are inherent weaknesses in this model. The Inverse Radius fit provided an improved alternative to the 2D Gaussian fit, with a better match with the data and more accurate emissions estimates. The lifetime estimates were also closer to the model-specified chemical lifetimes, although they remain biased low. Finally, the EMG model has an excellent fit with the data and gives consistently better emissions estimates for stronger wind cases than the box model and the 2D Gaussian fit. The lifetime estimates are also much closer to the model-specified chemical lifetimes, although these are quite sensitive to the accuracy of the plume rotation. Separate tests not presented here found that the best plume rotation algorithm (those that produce the narrowest time-averaged plume) led to the longest lifetimes. Estimates of plume rotation based on wind direction rather than plume direction led to shorter estimates of the chemical lifetime. Comparing the realistic wind cases with the synthetic cases suggests that increasing wind variability decreases the accuracy of the methods and leads to shorter lifetime estimates. This could lead to diurnal variations in the robustness of the estimates, an issue which should be explored in the context of future geostationary satellite missions which will provide diurnal profiles of columns.

4. Conclusions

Table 3 provides a summary of the evaluation of the four emissions estimation methods tested in this paper: 1. the box model, 2. the 2D Gaussian fit, 3. the Inverse Radius fit, and 4. the Exponentially-Modified Gaussian fit. As discussed above, all emissions estimates have a linear dependence on the estimate of the plume transport speed which can lead to increased errors.

The box model is found to give estimates within 5–20% of the model-specified value depending on the uncertainty in wind speeds. The estimates themselves are fairly robust to variations in both the wind speeds and the wind direction. If the chemical lifetime is known, then it can be included in the model to obtain emissions estimates even in cases with chemical reactions. Note however that uncertainties in the chemical lifetime estimates will add to the uncertainties in the emissions estimates. In the case of NO_x this could lead to systematic biases due for example to uncertainties in the partitioning between NO and NO_2 or between PAN and NO_x.

Table 3
Summary of the strengths and weaknesses of the four methods for estimating emissions and lifetimes, and requirements for improving the estimates.

	Box model	2D Gaussian fit	Inverse radius fit	EMG fit
Emissions estimate	All emissions estimates are linearly dependent on the estimate of the plume speed			
Plume speeds	Robust	Speed-dependent bias	Robust	Stronger winds
Plume direction	Robust	Omnidirectional	Omnidirectional	Accurate plume rotation
Sensitivity to chemistry	Required on input	τ-dependent bias	Fairly robust	Somewhat robust
Lifetime estimate	Model input	Dispersion, very short	Chemical, biased low	Chemical, biased low

The 2D Gaussian fit provides estimates within 30–40% of the model-specified value so long as the plume dispersion takes place in all directions. Comparison of the cross-sections with simulated column densities shows that the analytical solution is not a perfect match of the data even for the synthetic case. This leads to systematic discrepancies between the data and the fit, such that the results of the method can depend on factors like the domain selected for optimization. The method is somewhat robust to chemical lifetimes, but the lifetime estimate is always very short, reflecting the dispersion time from the source rather than the chemical lifetime in the plume.

The Inverse Radius fit matched the data much more closely, and yielded emissions estimates that were within 10–25% of the model-specified value. The method performed best with stronger winds and omnidirectional plume dispersion. The lifetime estimates were much closer to the model-specified chemical lifetime than the 2D Gaussian fit, although they were still biased low for the results using 2005 meteorology compared with the synthetic data.

Along with the Inverse Radius fit, the EMG fit provided the best estimates across the range of wind speed groups and conditions, and across the different chemical cases. The stronger wind cases were consistently the best, with results within 5–7% of the model-specified value for the slow chemistry cases and underpredicted by 15% for the 1-h chemistry case. Furthermore, the EMG fit can provide accurate estimates of the chemical lifetime in the plume. The lifetime estimate is however quite sensitive to the wind speed group, and also to inaccuracies in the plume rotation algorithm. This means that when applying the method particular care must be exercised in rotating the column densities, in grouping the times to be included in the analysis and in interpreting the results.

This study was based on model results and therefore provides an upper bound on the accuracy of the methods presented. When using satellite data, there will be additional uncertainties that can be expected to increase the errors in the estimates. For example there will be less data available, missing data and variable grid resolution that could all reduce the performance. The presence of multiple sources in proximity to each other as well as variable background levels can both complicate the analysis. The resolution in the vertical and the need to consider averaging kernels will further add to the uncertainty. The study was also limited to a single point source, it is likely that the uncertainties will increase when dealing with area sources such as urban areas. Nonetheless, the results suggest that useful estimates can be made of emissions and lifetimes from column density data provided that certain conditions are met to optimize those estimates.

Acknowledgments

This research was funded by the NASA Air Quality Applied Sciences Team (AQAST) program, NASA grant #NNX11AJ63G, including funding for the AQAST Tiger Team “Relationships and trends among satellite NO_2 columns, NO_x emissions, and air quality in North America.” We are grateful for valuable comments and discussion from the team members and the team leader and assistant leader, Daniel J. Jacob and Tracey Holloway. We are also grateful for detailed reviewer comments that improved the quality of the paper.

References

Beirle, S., Platt, U., Von Glasow, R., Wenig, M., Wagner, T., 2004a. Estimate of nitrogen oxide emissions from shipping by satellite remote sensing. Geophys. Res. Lett. 31.

Beirle, S., Platt, U., Wenig, M., Wagner, T., 2004b. Highly resolved global distribution of tropospheric NO_2 using GOME narrow swath mode data. Atmos. Chem. Phys. 4, 1913–1924.

Beirle, S., Boersma, K.F., Platt, U., Lawrence, M.G., Wagner, T., 2011. Megacity emissions and lifetimes of nitrogen oxides probed from space. Science 333, 1737–1739.

Carn, S.A., Krueger, A.J., Krotkov, N.A., Yang, K., Levelt, P.F., 2007. Sulfur dioxide emissions from Peruvian copper smelters detected by the ozone monitoring instrument. Geophys. Res. Lett. 34, L09801.

Duncan, B.N., Yoshida, Y., de Foy, B., Lamsal, L.N., Streets, D.G., Lu, Z., Pickering, K.E., Krotkov, N.A., 2013. The observed response of ozone monitoring instrument (OMI) NO_2 columns to NO_x emission controls on power plants in the United States: 2005–2011. Atmos. Environ. 81, 102–111.

ENVIRON, 2011. CAMx User's Guide, Comprehensive Air Quality Model with EXtensions. Technical Report Version 5.40. ENVIRON International Corporation.

Fioletov, V., McLinden, C., Krotkov, N., Moran, M., Yang, K., 2011. Estimation of SO_2 emissions using OMI retrievals. Geophys. Res. Lett. 38.

Fioletov, V., McLinden, C., Krotkov, N., Yang, K., Loyola, D., Valks, P., Theys, N., Van Roozendael, M., Nowlan, C., Chance, K., et al., 2013. Application of OMI, SCIAMACHY, and GOME-2 satellite SO_2 retrievals for detection of large emission sources. J. Geophys. Res. Atmos. 118, 11–399.

Fishman, J., Iraci, L., Al-Saadi, J., Chance, K., Chavez, F., Chin, M., Coble, P., Davis, C., DiGiacomo, P., Edwards, D., et al., 2012. The United States' next generation of atmospheric composition and coastal ecosystem measurements. Bull. Am. Met. Soc. 93.

de Foy, B., Krotkov, N.A., Bei, N., Herndon, S.C., Huey, L.G., Martínez, A.P., Ruiz-Suárez, L.G., Wood, E.C., Zavala, M., Molina, L.T., 2009. Hit from both sides: tracking industrial and volcanic plumes in mexico city with surface measurements and OMI SO_2 retrievals during the MILAGRO field campaign. Atmos. Chem. Phys. 9, 9599–9617.

de Foy, B., Cui, Y.Y., Schauer, J.J., Janssen, M., Turner, J.R., Wiedinmyer, C., 2014a. Estimating sources of elemental and organic carbon and their temporal emission patterns using a least squares inverse model and hourly measurements from the St. Louis – Midwest Supersite. Atmos. Chem. Phys. Discuss. 14, 12019–12070.

de Foy, B., Heo, J., Schauer, J.J., 2014b. Estimation of direct emissions and atmospheric processing of reactive mercury using inverse modeling. Atmos. Environ. 85, 73–82.

Ghude, S.D., Kulkarni, S.H., Jena, C., Pfister, G.G., Beig, G., Fadnavis, S., van der, A.,R., 2013. Application of satellite observations for identifying regions of dominant sources of nitrogen oxides over the Indian subcontinent. J. Geophys. Res. Atmos. 118, 1075–1089.

Hilsenrath, E., Chance, K., 2013. NASA ups the TEMPO on monitoring air pollution. Earth Obs. 25, 10–16.

Hoff, R.M., Christopher, S.A., 2009. Remote sensing of particulate pollution from space: have we reached the promised land? J. Air Waste Manage. Assoc. 59, 645–675.

Jacob, D.J., 1999. Introduction to Atmospheric Chemistry. Princeton University Press.

Lamsal, L., Martin, R., Van Donkelaar, A., Steinbacher, M., Celarier, E., Bucsela, E., Dunlea, E., Pinto, J., 2008. Ground-level nitrogen dioxide concentrations inferred from the satellite-borne ozone monitoring instrument. J. Geophys. Res. Atmos. 113.

Lamsal, L., Martin, R., Padmanabhan, A., van Donkelaar, A., Zhang, Q., Sioris, C., Chance, K., Kurosu, T., Newchurch, M., 2011. Application of satellite observations for timely updates to global anthropogenic NO_x emission inventories. Geophys. Res. Lett. 38.

Lee, C., Martin, R.V., van Donkelaar, A., Lee, H., Dickerson, R.R., Hains, J.C., Krotkov, N., Richter, A., Vinnikov, K., Schwab, J.J., 2011. SO_2 emissions and lifetimes: estimates from inverse modeling using in situ and global, space-based (SCIAMACHY and OMI) observations. J. Geophys. Res. Atmos. 116.

Leue, C., Wenig, M., Wagner, T., Klimm, O., Platt, U., Jähne, B., 2001. Quantitative analysis of NO_x emissions from global ozone monitoring experiment satellite image sequences. J. Geophys. Res. Atmos. 106, 5493–5505.

Lu, Z., Streets, D.G., 2012. Increase in NO_x emissions from Indian thermal power plants during 1996–2010: unit-based inventories and multisatellite observations. Environ. Sci. Technol. 46, 7463–7470.

Lu, Z., Streets, D.G., de Foy, B., Krotkov, N.A., 2013. Ozone monitoring instrument observations of interannual increases in SO_2 emissions from Indian coal-fired power plants during 2005–2012. Environ. Sci. Technol. 47, 13993–14000.

Martin, R.V., 2008. Satellite remote sensing of surface air quality. Atmos. Environ. 42, 7823–7843.

Martin, R.V., Jacob, D.J., Chance, K., Kurosu, T.P., Palmer, P.I., Evans, M.J., 2003. Global inventory of nitrogen oxide emissions constrained by space-based observations of NO_2 columns. J. Geophys. Res. Atmos. 108, 4537–4548.

Mesinger, F., DiMego, G., Kalnay, E., Mitchell, K., Shafran, P., Ebisuzaki, W., Jovic, D., Woollen, J., Rogers, E., Berbery, E., Ek, M., Fan, Y., Grumbine, R., Higgins, W., Li, H., Lin, Y., Manikin, G., Parrish, D., Shi, W., 2006. North american regional reanalysis. Bull. Amer. Met. Soc. 87, 343.

Russell, A.R., Valin, L.C., Bucsela, E.J., Wenig, M.O., Cohen, R.C., 2010. Space-based constraints on spatial and temporal patterns of NO_x emissions in California, 2005–2008. Environ. Sci. Technol. 44, 3608–3615.

Skamarock, W.C., Klemp, J.B., Dudhia, J., Gill, D.O., Barker, D.M., Wang, W., Powers, J.G., 2005. A Description of the Advanced Research WRF Version 2. Technical Report NCAR/TN-468+STR. NCAR.

Streets, D.G., Canty, T., Carmichael, G.R., de Foy, B., Dickerson, R.R., Duncan, B.N., Edwards, D.P., Haynes, J.A., Henze, D.K., Houyoux, M.R., et al., 2013. Emissions estimation from satellite retrievals: a review of current capability. Atmos. Environ. 77, 1011–1042.

Streets, D.G., de Foy, B., Duncan, B.N., Lamsal, L.N., Li, C., Lu, Z., February 2014. Using satellite observations to measure power plant emissions and their trends. Environ. Manag. (em), 16–21.

Sutton, O., 1932. A theory of eddy diffusion in the atmosphere. Proc. R. Soc. Lond. A, 143–165.

Valin, L., Russell, A., Hudman, R., Cohen, R., 2011. Effects of model resolution on the interpretation of satellite NO_2 observations. Atmos. Chem. Phys. 11, 11647–11655.

Valin, L., Russell, A., Cohen, R., 2013. Variations of oh radical in an urban plume inferred from NO_2 column measurements. Geophys. Res. Lett. 40, 1856–1860.

Vinken, G., Boersma, K., van Donkelaar, A., Zhang, L., 2014. Constraints on ship NO_x emissions in europe using GEOS-Chem and OMI satellite NO_2 observations. Atmos. Chem. Phys. 14, 1353–1369.